A&A 669, L9 (2023)
https://doi.org/10.1051/0004-6361/202245448

Astronomy & Astrophysics

LETTER TO THE EDITOR

Higher metal abundances do not solve the solar problem

G. Buldgen[1,2], P. Eggenberger[1], A. Noels[2], R. Scuflaire[2], A. M. Amarsi[3], N. Grevesse[2,4], and S. Salmon[1]

[1] Département d'Astronomie, Université de Genève, Chemin Pegasi 51, 1290 Versoix, Switzerland
e-mail: Gael.Buldgen@unige.ch
[2] STAR Institute, University of Liège, 19C Allée du 6 Août, 4000 Liège, Belgium
[3] Theoretical Astrophysics, Department of Physics and Astronomy, Uppsala University, Box 516, 751 20 Uppsala, Sweden
[4] Centre Spatial de Liège, Université de Liège, Avenue Pré Aily, 4031 Angleur-Liège, Belgium

Received 12 November 2022 / Accepted 12 December 2022

ABSTRACT

Context. The Sun acts as a cornerstone of stellar physics. Thanks to spectroscopic, helioseismic and neutrino flux observations, we can use the Sun as a laboratory of fundamental physics in extreme conditions. The conclusions we draw are then used to inform and calibrate evolutionary models of all other stars in the Universe. However, solar models are in tension with helioseismic constraints. The debate on the 'solar problem' has hitherto led to numerous publications discussing potential issues with solar models and abundances.
Aims. Using the recently suggested high-metallicity abundances for the Sun, we compute standard solar models as well as models with macroscopic transport that reproduce the solar surface lithium abundances, and we analyze their properties in terms of helioseismic and neutrino flux observations.
Methods. We compute solar evolutionary models and combine spectroscopic and helioseismic constraints as well as neutrino fluxes to investigate the impact of macroscopic transport on these measurements.
Results. When high-metallicity solar models are calibrated to reproduce the measured solar lithium depletion, tensions arise with respect to helioseismology and neutrino fluxes. This is yet another demonstration that the solar problem is also linked to the physical prescriptions of solar evolutionary models and not to chemical composition alone.
Conclusions. A revision of the physical ingredients of solar models is needed in order to improve our understanding of stellar structure and evolution. The solar problem is not limited to the photospheric abundances if the depletion of light elements is considered. In addition, tighter constraints on the solar beryllium abundance will play a key role improving of solar models.

Key words. Sun: helioseismology – Sun: oscillations – Sun: fundamental parameters – Sun: abundances

1. Introduction

The Sun plays a key role in stellar physics. Thanks to the numerous high-quality observations available, it acts as both a laboratory of fundamental physics and a calibrator for stellar evolution models (Christensen-Dalsgaard 2021). However, the modelling of solar structure is still a subject of debate, fuelled in part by uncertainties in the solar chemical composition. Striking disagreements exist with helioseismic constraints, when the 'low-metallicity' compositions presented in Asplund et al. (2005, 2009), and more recently in Asplund et al. (2021) and Amarsi et al. (2021) are adopted – hereafter, the 'solar problem' (see e.g., Basu & Antia 2008; Buldgen et al. 2019a, and references therein). These low-metallicity compositions are based on spectroscopic analyses of the solar disc-centre intensity, and use 3D radiative-hydrodynamic (RHD) simulations of the solar atmosphere and, where available, non-local thermodynamic equilibrium (non-LTE) radiative transfer.

Recently, Magg et al. (2022) presented a new spectroscopic analysis of the solar chemical composition. In contrast to the papers cited above, their analysis was based on the solar disc-integrated flux (in which spectral lines form higher up in the atmosphere and are thus potentially more sensitive to non-LTE effects as well as to blends that can be exacerbated by the extra broadening due to rotation) and 1D model atmospheres (derived from spatial and temporal averages of 3D RHD models). They inferred a 'high-metallicity' chemical composition similar to the canonical 1D LTE compilations of Grevesse & Noels (1993) and Grevesse & Sauval (1998), hereafter GN93 and GS98. Using this high-metallicity composition and standard solar models (SSMs), they find better agreement with helioseismic constraints. They concluded that the solar problem is solved, without the need for any revision of fundamental physical ingredients.

We consider whether the solar problem is in fact solved. We show that a revision of abundances simply affects the magnitude of the corrections required in solar models, but does not validate a physical prescription for modelling the Sun. Recently, Eggenberger et al. (2022) demonstrated that stepping away from the SSMs is required to simultaneously reproduce both helioseismic inversions of the solar internal rotation and the spectroscopic measurement of the lithium photospheric abundance; a result that was foreseen by Christensen-Dalsgaard et al. (1996). In the last few decades, numerous studies have investigated the implications of revising the physical ingredients of solar models, such as accretion, mass loss, the transport of chemicals, convection, opacities, dark matter, dark energy and nuclear reactions (see e.g., Guzik et al. 2001, 2005; Brun et al. 2002; Guzik & Mussack 2010; Vinyoles et al. 2015; Spada et al. 2018; Zhang et al. 2019;

Bellinger & Christensen-Dalsgaard 2022; Saltas & Christensen-Dalsgaard 2022; Yang 2019, 2022, and references therein) and multiple generations of standard and non-standard models were computed (e.g., Serenelli 2010; Vinyoles et al. 2017; Christensen-Dalsgaard et al. 2018; Jørgensen & Weiss 2018, amongst other).

We focus on the changes induced by reproducing the lithium abundance with various parametric diffusion coefficients using solar models built with the Magg et al. (2022) abundances, similarly to Richard et al. (1996). We discuss the impact on neutrino fluxes and the helioseismic constraints of reproducing all available spectroscopic constraints and how improved beryllium abundances will help us pin down the properties of macroscopic transport at the base of the solar convective zone (BCZ).

2. Standard and non-standard solar models

We present our set of solar evolutionary models and discuss the changes in properties induced by the inclusion of macroscopic transport at the BCZ. We used both SSMs and non-standard models, computed with the Liège Stellar Evolution Code (Scuflaire et al. 2008). We used the following physical ingredients: the solar abundances from Magg et al. (2022), Opacity Project (OP) opacities (Badnell et al. 2005), supplemented at low temperature by opacities from Ferguson et al. (2005), the FreeEOS equation of state (Irwin 2012), and nuclear reaction rates from Adelberger et al. (2011).

The first model, Model Std, is a SSM and includes microscopic diffusion following Thoul et al. (1994), with the screening coefficients of Paquette et al. (1986) and the effects of partial ionization. As seen from Table 1, the results for this setup are almost identical to those illustrated in Table 6 of Magg et al. (2022). The slight differences in the positioning of the BCZ are due to differences in the prescription for microscopic diffusion that can alter the metallicity profile close to the BCZ (see also Table 1 in Buldgen et al. 2019b for an illustration).

All other models in Table 1 were computed with an additional parametric diffusion coefficient, with the aim of reproducing the solar lithium abundance (Wang et al. 2021). To do so, we assumed the initial lithium and beryllium abundances to be equal to the meteoritic values (Lodders et al. 2009). We started with Model DT_R, which we fitted to reproduce the transport induced by the combined effect of shear-induced turbulence, meridional circulation and the magnetic Tayler instability (Eggenberger et al. 2022). We adopted a simple power-law parametrization of the density following Proffitt & Michaud (1991)

$$D_T(r) = D\left(\frac{\rho_{\rm BCZ}}{\rho(r)}\right)^n, \quad (1)$$

with D a constant in cm^2 s^{-1}, ρ the local value of the density, $\rho_{\rm BCZ}$ the value of the density at the BCZ of the model and n a fixed constant number. In their recent paper, Eggenberger et al. (2022) find that the behaviour of rotating models can be well reproduced with $n = 1.3$, which is used in Model DT_R. In addition, we also tested different values of n, from 2 to 5, to investigate the impact of reproducing the solar lithium depletion in solar models. We note that the depletion is highly significant, as lithium is reduced by 2.29 dex with an uncertainty on the current photospheric abundance of 0.06 dex. Therefore it constitutes an important constraint to consider when studying solar evolution.

The results of the calibrated models with parametric transport are provided in Table 1. The BCZ position in the model is altered when macroscopic mixing is included, and thus we investigated in model $DT_R + Ov$ the effect of including adiabatic overshooting to replace the transition in temperature gradient at the helioseismic value of $0.713 \pm 0.001\,R_\odot$ (Basu & Antia 1997).

Table 1. Parameters of the solar evolutionary models.

Name	$(r/R)_{\rm BCZ}$	$(m/M)_{\rm CZ}$	$Y_{\rm CZ}$
Model Std	0.7148	0.9760	0.2443
Model DT_R	0.7182	0.9769	0.2522
Model DT_2	0.7178	0.9768	0.2513
Model DT_3	0.7177	0.9768	0.2510
Model DT_4	0.7176	0.9768	0.2507
Model DT_5	0.7174	0.9767	0.2503
Model $DT_R + Ov$	0.7133	0.9759	0.2516

The following sections discuss the results obtained and their consequences for the current issues in solar modelling.

3. Lithium, helium, neutrinos and convective envelope position

The evolution of the photospheric lithium and beryllium abundances as a function of the solar age are shown in Fig. 1, with $A(X) = \log(X/{\rm H}) + 12$. A first result confirmed here is that SSMs are unable to reproduce the lithium depletion in the Sun. As mentioned in Proffitt & Michaud (1991), additional mixing at the BCZ is required to reproduce the observed depletion.

The calibration of this mixing was done for various values of n, changing the value of D simultaneously to reproduce the lithium abundance. Each leads to a different beryllium depletion at the age of the Sun. In the right panel of Fig. 1, we show that a higher value of n leads to a lower depletion of beryllium at the age of the Sun. This is a direct consequence of the higher burning temperature of beryllium at $\approx 3.5 \times 10^6$ K. A higher n value leads to a steeper diffusion coefficient and thus a less efficient transport of beryllium down to $\approx 3.5 \times 10^6$ K, despite the recalibration of the factor D to reproduce the lithium depletion. Thus beryllium acts as a strong constraint on the functional form of the macroscopic transport coefficient at the BCZ and is thus of highest importance for constraining the physical origin of the lithium depletion.

The final beryllium abundance will also be affected by the presence or absence of strong adiabatic overshooting at the BCZ. The inclusion of this additional mixing has strong consequences for solar models. First, the position of the BCZ is significantly shifted by about $0.002\,R_\odot$ (hence 2σ) with respect to the position obtained in the SSM framework. This shift is also linked to a small change in the mass coordinate of the convective zone. It is actually due to a change in the metallicity profile close to the BCZ. When only microscopic diffusion is included in the models, the competition between pressure diffusion and thermal diffusion leads to a drop in diffusion velocities close to the BCZ that induces an accumulation of elements (see Baturin et al. 2006, for a discussion).

This is particularly visible for the Z profile of SSMs. The accumulation of metals close to the BCZ locally increases the opacity, as the main contributors at the BCZ are oxygen, iron and neon. Therefore, the temperature gradient is locally steepened, leading to a deeper convective zone. Once macroscopic transport is included in the models, this local maximum is erased, which leads to a shallower convective zone. This result is obtained for

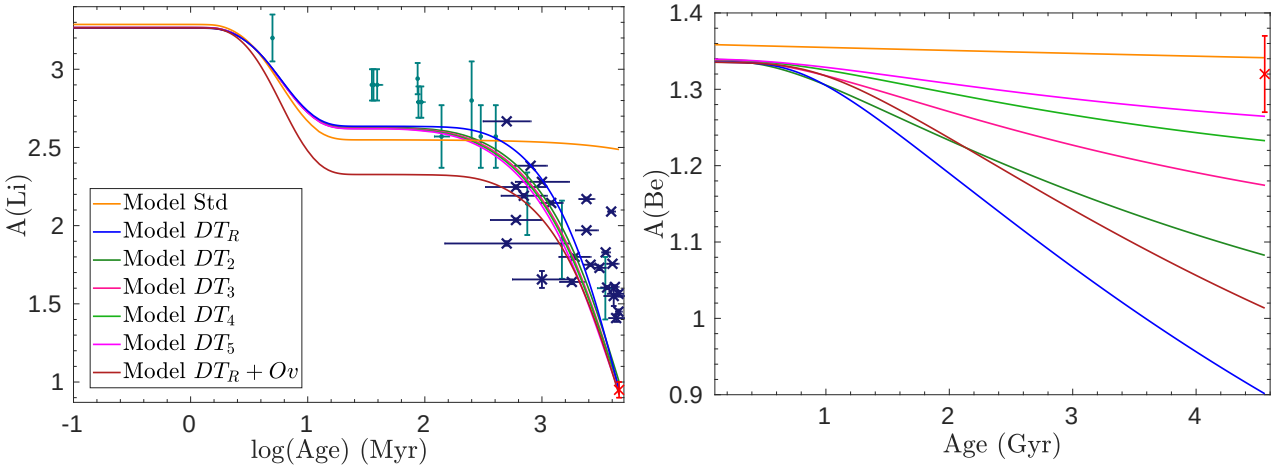

Fig. 1. Left panel: lithium photosperic abundance as a function of age for the models in Table 1. The red cross is the solar value and the dark blue and teal crosses are the values for young solar-like stars in open clusters from Dumont et al. (2021). Right panel: beryllium photospheric abundance as a function of age for the models in Table 1. The red cross indicates the solar value from Asplund et al. (2009).

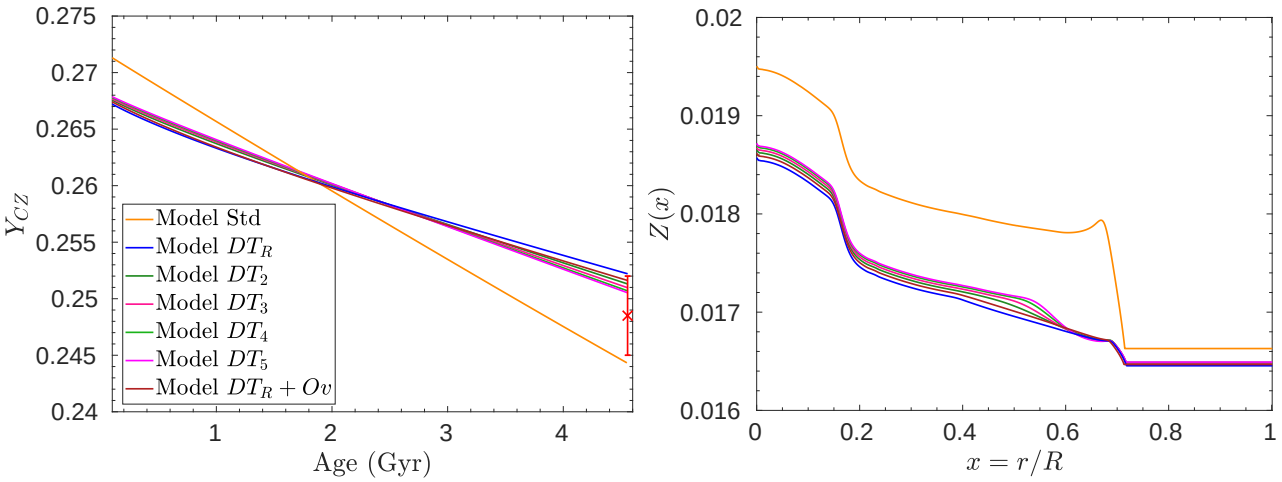

Fig. 2. Left panel: evolution of the helium abundance in the convective zone Y_{CZ} for the evolutionary models in Table 1. The red cross indicates the seismic value and the 1σ interval from Basu & Antia (1995). Right panel: metallicity profile as a function of normalized radius for the evolutionary models in Table 1.

all models that include transport with a $n \leq 5$. From Fig. 2, we can see that n should be much higher than 5 to avoid this issue, meaning that D should be increased significantly to compensate and the transport should probably behave almost instantaneously in a shallow region, coming closer to the behaviour of the model with overshooting and showing tension with the results of young solar-like stars in open clusters (taken from Dumont et al. 2021). Meanwhile, beryllium would provide a definitive answer as to the behaviour of the mixing and thus its physical origin.

A second consequence of the inclusion of macroscopic mixing is the reduction of the efficiency of gravitational settling. As the microscopic diffusion velocities drop very fast in the radiative interior, if mixing is included, settling is inhibited, as seen in Fig. 2. To reproduce the solar luminosity and radius at the solar age, a higher initial hydrogen abundance is required and thus the core metallicity at the age of the Sun is reduced.

Due to the lower core metallicity, neutrino fluxes are significantly affected, as shown in Table 2. The pp flux, $\phi_{\rm pp}$, is unchanged as it is mostly related to reproducing the solar luminosity. The beryllium and boron neutrino fluxes, $\phi_{\rm Be}$ and $\phi_{\rm B}$, are significantly affected by the inclusion of macroscopic transport, as the core metallicity, temperature and temperature gradient are not high enough and steep enough to reproduce the observations. We refer the reader to Salmon et al. (2021) for an in-depth discussion in the case of SSM using various physical ingredients as well as to the seminal works by Bahcall et al. (2005), Bahcall & Serenelli (2005) and to Villante & Serenelli (2021) for a review. Similarly, the CNO neutrino flux is significantly reduced and now in disagreement with the observed value from the Borexino experiment (Borexino Collaboration 2022). Therefore, additional processes such as planetary formation (Kunitomo & Guillot 2021; Kunitomo et al. 2022), or a modification to key physical ingredients such as opacity or the electronic screening formalism (Mussack & Däppen 2011; Mussack 2011), might be required to reproduce the neutrino observations when the lithium depletion is reproduced, particularly the fluxes from Borexino.

Another consequence of the inhibition of settling seen from the left panel of Fig. 2 is that the mass fraction value of Helium in the solar convective (CZ) is significantly changed. While it was in marginal disagreement with the lower end of the helioseismically inferred interval in the SSM, it is now in marginal

Table 2. Neutrino fluxes of the evolutionary models.

Name	ϕ(pp)	ϕ(Be)	ϕ(B)	ϕ(CNO)
Model Std	5.96	4.89	5.42	6.11
Model DT_R	5.98	4.73	5.04	5.53
Model DT_2	5.98	4.74	5.07	5.57
Model DT_3	5.98	4.75	5.08	5.59
Model DT_4	5.98	4.75	5.09	5.61
Model DT_5	5.98	4.76	5.10	5.63
Model $DT_R + Ov$	5.98	4.74	5.06	5.56
O-G21[1]	$5.97^{+0.0037}_{-0.0033}$	$4.80^{+0.24}_{-0.22}$	$5.16^{+0.13}_{-0.09}$	–
Borexino[2]	$6.1^{+0.6}_{-0.7}$	$4.99^{+0.13}_{-0.14}$	$5.68^{+0.39}_{-0.41}$	$6.6^{+2.0}_{-0.9}$

Notes. [1]Orebi Gann et al. (2021), [2]Borexino Collaboration (2018, 2020, 2022).

agreement or disagreement with the upper end of the interval in the models with transport. This impacts the agreement with the first adiabatic exponent profile, $\Gamma_1 = \frac{\partial \ln P}{\partial \ln \rho}|_S$, in the solar convective envelope determined from helioseismology. As seen from Vorontsov et al. (2013; e.g., Figs. 6 and 7), a helium mass fraction above 0.25 is never in agreement with a metal mass fraction above 0.012, whatever the equation of state used. Further investigations of the properties of the Γ_1 profile in the solar envelope with the most recent equations of state are required to restrict the Y–Z interval allowed in solar models, as this would provide strong constraints on the transport of chemical elements during solar evolution.

4. Helioseismic inversions

The second point to investigate is the impact of transport on helioseismic inversions. As shown in Magg et al. (2022), the increased metallicity brought the models back to the level of agreement of the SSMs of the 1990s. As shown in the left panel of Fig. 3, we reach similar conclusions. In the right panel of Fig. 3, we illustrate the inversion result for the entropy proxy, $S_{5/3} = P/\rho^{5/3}$, introduced in Buldgen et al. (2017b), which provides a complementary view of solar models. The level of agreement of the standard model is excellent and similar to that of the GS98 or GN93 models in Buldgen et al. (2019b). This is no surprise as the Magg et al. (2022) abundances are almost the same as the GS98 abundances. They are, however, in strong disagreement with the surface lithium abundance.

The models based on high-metallicity abundances that are able to reproduce the surface lithium abundance draw a more complex picture. As illustrated in previous works (e.g., Brun et al. 2002; Christensen-Dalsgaard et al. 2011, 2018), macroscopic transport reduces the glitch at the BCZ, but also leads to increased discrepancies in the deeper radiative zone and in the core. While still small, they remain significant. From the entropy proxy inversions, we see that macroscopic transport does not improve the agreement with helioseismic inversions. The entropy plateau in the convective zone is now too high, and some deviations are seen in the radiative zone, particularly at the BCZ due to the less steep temperature gradient induced by the erasement of the metallicity peak resulting from microscopic diffusion. This further emphasizes the tension between the models including macroscopic transport and constraints such as neutrino fluxes and helioseismic inversions.

Overall, the results simply illustrate the importance of putting helioseismic inversions in their context. The final sound speed and entropy proxy profiles will be the result of the whole calibration procedure and therefore of all the ingredients entering the model computation.

The only way to directly constrain the solar metallicity using helioseismology is by using Γ_1, which is highly sensitive to the equation of state of the solar plasma and has a tendency to favour a low-metallicity (Vorontsov et al. 2013; Buldgen et al. 2017a) value in the most recent studies. Therefore, determining solely the solar metallicity from helioseismic data is currently restricted by the data available (further analyses using the sets of modes from Reiter et al. 2020 are required) and by the reliability of the solar equation of state in the deep convective envelope.

5. Conclusion

In this study, we have discussed in detail the implications of the physical ingredients of solar models regarding the conclusion of the solar problem in light of the high-metallicity composition presented by Magg et al. (2022). We have shown that, as it stands, further constraints on the solar beryllium abundance are key to better understanding the properties of macroscopic transport at the BCZ. We have also shown that SSMs are in complete disagreement with the observed solar lithium abundance. However, our work only tackles one aspect of the issue, following previous works (e.g., Richard et al. 1996; Brun et al. 2002; Christensen-Dalsgaard et al. 2018; Zhang et al. 2019), and numerous other processes can be demonstrated to impact the results of comparisons between solar models and helioseismic constraints, as shown in the extensive literature on the subject (see Christensen-Dalsgaard 2021, and references therein).

One solution to erase this disagreement is to introduce macroscopic transport at the base of the envelope, which could originate in the combined actions of rotation and magnetic instabilities, as shown in Eggenberger et al. (2022). We tested various parametrizations and their impact on various key constraints of solar models. We find the following:

- The inclusion of macroscopic transport leads to tension with the helioseismic Y_{CZ} value, as well as with the Γ_1 profile inversions of Vorontsov et al. (2013). Looking at the results of Table 1 in Buldgen et al. (2019b), using other key ingredients such as the OPAL opacities or the SAHA-S equation of state might lead to a higher Y value, which would further increase these tensions.
- The r_{CZ} value is significantly impacted by the inclusion of macroscopic transport to reproduce the photospheric lithium abundance, leading to a shift by about 2σ of its position. We also note that it is significantly affected by the physical prescription used for microscopic diffusion.
- Some tension is also observed with the lithium abundance of young solar twins in stellar clusters. Repositioning r_{CZ} at the helioseismic value using adiabatic overshooting further increases this tension.
- By changing the initial conditions of the calibration, macroscopic transport also leads to a significantly lower Z abundance in the core, in turn leading to tension with the CNO Borexino neutrino fluxes and disagreement with the beryllium and boron fluxes at 1σ level.
- Sound speed and entropy proxy profiles in the solar interior are overall worse when macroscopic transport is included.

In their work, Magg et al. (2022) conclude that 'While SSMs offer an incomplete description of the physics in the solar interior, current results alleviate the need for more complex physics, such as accretion of metal-poor material (Serenelli et al. 2011), energy transport by dark matter particles (Vincent et al. 2015),

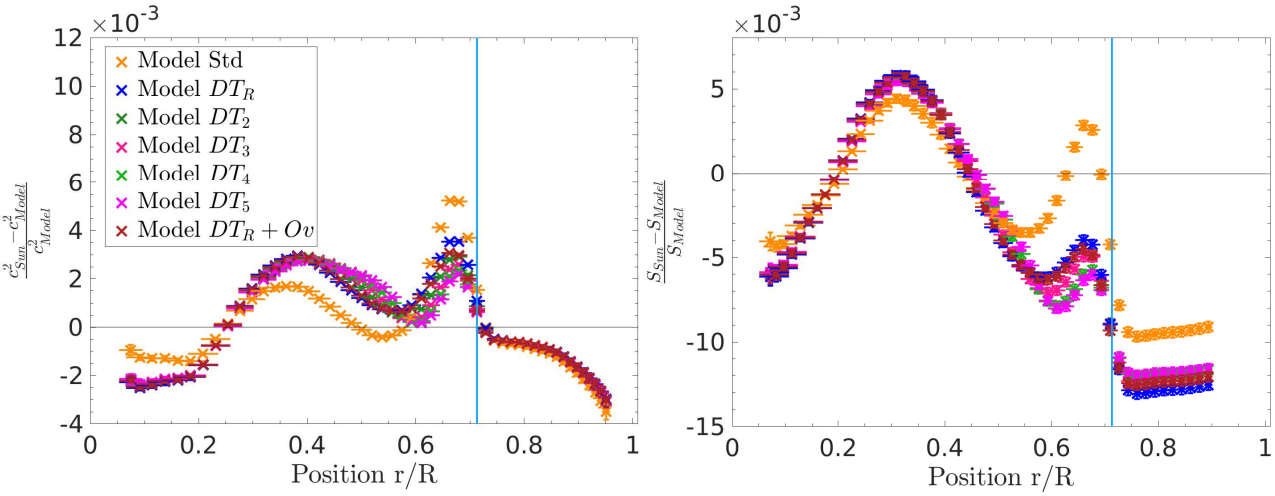

Fig. 3. Left panel: relative differences in squared adiabatic sound speed between the Sun and the evolutionary models in Table 1. Right panel: relative differences in entropy proxy between the Sun and the evolutionary models in Table 1.

revision of opacities (Bailey et al. 2015), enhanced gravitational settling and other effects (Guzik & Mussack 2010).'. We find this assessment to be incorrect, as reproducing the lithium abundance with various parametrizations essentially reduces and even destroys the agreement they find for some constraints.

The situation for solar models using the Asplund et al. (2021) abundances is going to be slightly different. Including transport helps reproduce the helium abundance in the CZ (Yang 2019, 2022; Eggenberger et al. 2022) and agrees with Γ_1 inferences by Vorontsov et al. (2013). However, it does not solve the issues with the positioning of the BCZ, the sound speed profile and the neutrino fluxes. Those will likely require revision of physical ingredients. Ultimately, the only difference between the Asplund et al. (2021) models and the Magg et al. (2022) models is the required magnitude of these revisions.

Therefore, we find that the need for additional physics such as the effects of rotation, of which we have a clear map (e.g., Schou et al. 1998), planetary formation, of which the impact can be measured (Kunitomo & Guillot 2021; Kunitomo et al. 2022) and opacity revision, which can be quantified and tested (e.g., Ayukov & Baturin 2017; Buldgen et al. 2019b) is not alleviated. On the contrary, the discussion related to the metal content of the Sun cannot be separated from other fundamental physical ingredients used in solar models such as the equation of state, the radiative opacities, the transport of chemicals or the evolutionary history. In this context, a further refining of the fundamental physics computations, experimental setups, and helioseismic techniques is paramount to providing the most accurate description of the internal structure of the Sun and using it as a stepping stone for the modelling of solar-like stars. Indeed, the need for additional transport at the base of convective envelopes is found in solar twins (Deal et al. 2015) and F-type stars (Verma & Silva Aguirre 2019) and often considered a key ingredient for determining reliable stellar ages. Continuing to explore such processes for our very own Sun thus appears a natural and meaningful endeavour.

Acknowledgements. We thank the referee for his/her useful comments that helped improving the manuscript. G.B. is funded by the SNF AMBIZIONE grant No 185805 (Seismic inversions and modelling of transport processes in stars). P.E. and S. J. A. J. S. have received funding from the European Research Council (ERC) under the European Union's Horizon 2020 research and innovation programme (grant agreement No 833925, project STAREX). A.M.A. gratefully acknowledges support from the Swedish Research Council (VR 2020-03940). We acknowledge support by the ISSI team "Probing the core of the Sun and the stars" (ID 423) led by Thierry Appourchaux.

References

Adelberger, E. G., García, A., Robertson, R. G. H., et al. 2011, Rev. Mod. Phys., 83, 195
Amarsi, A. M., Grevesse, N., Asplund, M., & Collet, R. 2021, A&A, 656, A113
Asplund, M., Grevesse, N., & Sauval, A. J. 2005, in Cosmic Abundances as Records of Stellar Evolution and Nucleosynthesis, eds. I. Barnes, G. Thomas, & F. N. Bash, ASP Conf. Ser., 336, 25
Asplund, M., Grevesse, N., Sauval, A. J., & Scott, P. 2009, ARA&A, 47, 481
Asplund, M., Amarsi, A. M., & Grevesse, N. 2021, A&A, 653, A141
Ayukov, S. V., & Baturin, V. A. 2017, Astron. Rep., 61, 901
Badnell, N. R., Bautista, M. A., Butler, K., et al. 2005, MNRAS, 360, 458
Bahcall, J. N., & Serenelli, A. M. 2005, ApJ, 626, 530
Bahcall, J. N., Serenelli, A. M., & Basu, S. 2005, ApJ, 621, L85
Bailey, J. E., Nagayama, T., Loisel, G. P., et al. 2015, Nature, 517, 3
Basu, S., & Antia, H. M. 1995, MNRAS, 276, 1402
Basu, S., & Antia, H. M. 1997, MNRAS, 287, 189
Basu, S., & Antia, H. M. 2008, Phys. Rep., 457, 217
Baturin, V. A., Gorshkov, A. B., & Ayukov, S. V. 2006, Astron. Rep., 50, 1001
Bellinger, E. P., & Christensen-Dalsgaard, J. 2022, MNRAS, 517, 5281
Borexino Collaboration (Agostini, M., et al.) 2018, Nature, 562, 505
Borexino Collaboration (Agostini, M., et al.) 2020, Nature, 587, 577
Borexino Collaboration (Appel, S., et al.) 2022, Phys. Rev. Lett., 129, 252701
Brun, A. S., Antia, H. M., Chitre, S. M., & Zahn, J. P. 2002, A&A, 391, 725
Buldgen, G., Salmon, S. J. A. J., Noels, A., et al. 2017a, MNRAS, 472, 751
Buldgen, G., Salmon, S. J. A. J., Noels, A., et al. 2017b, A&A, 607, A58
Buldgen, G., Salmon, S., & Noels, A. 2019a, Front. Astron. Space Sci., 6, 42
Buldgen, G., Salmon, S. J. A. J., Noels, A., et al. 2019b, A&A, 621, A33
Christensen-Dalsgaard, J. 2021, Liv. Rev. Sol. Phys., 18, 2
Christensen-Dalsgaard, J., Dappen, W., Ajukov, S. V., et al. 1996, Science, 272, 1286
Christensen-Dalsgaard, J., Monteiro, M. J. P. F. G., Rempel, M., & Thompson, M. J. 2011, MNRAS, 414, 1158
Christensen-Dalsgaard, J., Gough, D. O., & Knudstrup, E. 2018, MNRAS, 477, 3845
Deal, M., Richard, O., & Vauclair, S. 2015, A&A, 584, A105
Dumont, T., Palacios, A., Charbonnel, C., et al. 2021, A&A, 646, A48
Eggenberger, P., Buldgen, G., Salmon, S. J. A. J., et al. 2022, Nat. Astron., 6, 788
Ferguson, J. W., Alexander, D. R., Allard, F., et al. 2005, ApJ, 623, 585
Grevesse, N., & Noels, A. 1993, in Origin and Evolution of the Elements, eds. N. Prantzos, E. Vangioni-Flam, & M. Casse, 15
Grevesse, N., & Sauval, A. J. 1998, Space Sci. Rev., 85, 161
Guzik, J. A., & Mussack, K. 2010, ApJ, 713, 1108
Guzik, J. A., Neuforge-Verheecke, C., Young, A. C., et al. 2001, Sol. Phys., 200, 305
Guzik, J. A., Watson, L. S., & Cox, A. N. 2005, ApJ, 627, 1049

Irwin, A. W. 2012, Astrophysics Source Code Library [record ascl:1211.002]
Jørgensen, A. C. S., & Weiss, A. 2018, MNRAS, 481, 4389
Kunitomo, M., & Guillot, T. 2021, A&A, 655, A51
Kunitomo, M., Guillot, T., & Buldgen, G. 2022, A&A, 667, L2
Lodders, K., Palme, H., & Gail, H. P. 2009, Landolt Börnstein, 4B, 712
Magg, E., Bergemann, M., Serenelli, A., et al. 2022, A&A, 661, A140
Mussack, K. 2011, Ap&SS, 336, 111
Mussack, K., & Däppen, W. 2011, ApJ, 729, 96
Orebi Gann, G. D., Zuber, K., Bemmerer, D., & Serenelli, A. 2021, Ann. Rev. Nucl. Part. Sci., 71, 491
Paquette, C., Pelletier, C., Fontaine, G., & Michaud, G. 1986, ApJS, 61, 177
Proffitt, C. R., & Michaud, G. 1991, ApJ, 380, 238
Reiter, J., Rhodes, E. J., Jr, Kosovichev, A. G., et al. 2020, ApJ, 894, 80
Richard, O., Vauclair, S., Charbonnel, C., & Dziembowski, W. A. 1996, A&A, 312, 1000
Salmon, S. J. A. J., Buldgen, G., Noels, A., et al. 2021, A&A, 651, A106
Saltas, I. D., & Christensen-Dalsgaard, J. 2022, A&A, 667, A115
Schou, J., Antia, H. M., Basu, S., et al. 1998, ApJ, 505, 390
Scuflaire, R., Théado, S., Montalbán, J., et al. 2008, Ap&SS, 316, 83
Serenelli, A. M. 2010, Ap&SS, 328, 13
Serenelli, A. M., Haxton, W. C., & Peña-Garay, C. 2011, ApJ, 743, 24
Spada, F., Demarque, P., Basu, S., & Tanner, J. D. 2018, ApJ, 869, 135
Thoul, A. A., Bahcall, J. N., & Loeb, A. 1994, ApJ, 421, 828
Verma, K., & Silva Aguirre, V. 2019, MNRAS, 489, 1850
Villante, F. L., & Serenelli, A. 2021, Front. Astron. Space Sci., 7, 112
Vincent, A. C., Serenelli, A., & Scott, P. 2015, J. Cosmol. Astropart. Phys., 2015, 040
Vinyoles, N., Serenelli, A., Villante, F. L., et al. 2015, J. Cosmol. Astropart. Phys., 2015, 015
Vinyoles, N., Serenelli, A. M., Villante, F. L., et al. 2017, ApJ, 835, 202
Vorontsov, S. V., Baturin, V. A., Ayukov, S. V., & Gryaznov, V. K. 2013, MNRAS, 430, 1636
Wang, E. X., Nordlander, T., Asplund, M., et al. 2021, MNRAS, 500, 2159
Yang, W. 2019, ApJ, 873, 18
Yang, W. 2022, ApJ, 939, 61
Zhang, Q.-S., Li, Y., & Christensen-Dalsgaard, J. 2019, ApJ, 881, 103